Article:

Fogt, R.L., Goergens, C.A., Jones, J.M. et al. (2016) A twentieth century perspective on summer Antarctic pressure change and variability and contributions from tropical SSTs and ozone depletion. Geophysical Research Letters, 44 (19). pp. 9918-9927. ISSN: 0094-8276

https://doi.org/10.1002/2017GL075079

AGU PUBLICATIONS

Geophysical Research Letters

RESEARCH LETTER
10.1002/2017GL075079

Key Points:

- Only East Antarctica has significant negative summer pressure decreases since 1905
- The coastal South Atlantic sector of Antarctica displays positive summer pressure trends in the first half of the twentieth century
- Multiple factors, including tropical sea surface temperature variability, explain the recent negative summer Antarctic pressure trends

Supporting Information:

- Supporting Information S1

Correspondence to:
R. L. Fogt,
fogtr@ohio.edu

Citation:
Fogt, R. L., C. A. Goergens, J. M. Jones, D. P. Schneider, J. P. Nicolas, D. H. Bromwich, and H. E. Dusselier (2017), A twentieth century perspective on summer Antarctic pressure change and variability and contributions from tropical SSTs and ozone depletion, *Geophys. Res. Lett.*, *44*, 9918–9927, doi:10.1002/2017GL075079.

Received 25 JUL 2017
Accepted 25 AUG 2017

A twentieth century perspective on summer Antarctic pressure change and variability and contributions from tropical SSTs and ozone depletion

Ryan L. Fogt[1], Chad A. Goergens[1], Julie M. Jones[2], David P. Schneider[3], Julien P. Nicolas[4], David H. Bromwich[4,5], and Hallie E. Dusselier[1]

[1]Department of Geography and Scalia Laboratory for Atmospheric Analysis, Ohio University, Athens, Ohio, USA, [2]Department of Geography, University of Sheffield, Sheffield, UK, [3]National Center for Atmospheric Research, Boulder, Colorado, USA, [4]Polar Meteorology Group, Byrd Polar and Climate Research Center, Ohio State University, Columbus, Ohio, USA, [5]Atmospheric Sciences Program, Department of Geography, Ohio State University, Columbus, Ohio, USA

Abstract During the late twentieth century, the Antarctic atmospheric circulation has changed and significantly influenced the overall Antarctic climate, through processes including a poleward shift of the circumpolar westerlies. However, little is known about the full spatial pattern of atmospheric pressure over the Antarctic continent prior to 1979. Here we investigate surface pressure changes across the entire Antarctic continent back to 1905 by developing a new summer pressure reconstruction poleward of 60°S. We find that only across East Antarctica are the recent pressures significantly lower than pressures in the early twentieth century; we also discern periods of significant positive pressure trends in the early twentieth century across the coastal South Atlantic sector of Antarctica. Climate model simulations reveal that both tropical sea surface temperature variability and other radiative forcing mechanisms, in addition to ozone depletion, have played an important role in forcing the recent observed negative trends.

Plain Language Summary Since most Antarctic meteorological observations start around 1957, very little is known about atmospheric pressure variability across Antarctica throughout the entire twentieth century. Yet changes in the atmospheric circulation around Antarctica have been linked to warming across West Antarctica, the lack of warming in East Antarctica, and changes in the sea ice surrounding Antarctica. To better understand the significance of these changes in a historical context, a new spatially complete summer pressure reconstruction is generated and evaluated in this paper. Through the high quality of this reconstruction, we determine that only across East Antarctica are pressure changes significant when in context of the full twentieth century; over portions of the South Atlantic coastal sector of Antarctica, the early twentieth century was marked with pressure increases. Using a suite of climate model simulations, we determine that other factors, including tropical sea surface temperatures, are needed in order to fully replicate the recent negative summer pressure trends that have occurred across the entire continent. This work therefore highlights the role of natural variability in Antarctic pressure during the twentieth century, and the need to consider multiple mechanisms beyond ozone depletion to understand recent Antarctic pressure changes.

1. Introduction

Atmospheric surface pressure provides strong insight into Antarctic climate variability and change, given its dynamic relationship to the strength and direction of the winds, which influence patterns of thermal advection and sea ice variability. Several studies have indicated changes in atmospheric pressure across Antarctica since the late 1970s, including a positive trend in the Southern Annular Mode (SAM) [*Marshall*, 2003; *Jones et al.*, 2016], a deepening of the Amundsen Sea Low [*Turner et al.*, 2009, 2013; *Fogt and Zbacnik*, 2014; *Fogt and Wovrosh*, 2015; *England et al.*, 2016; *Raphael et al.*, 2016], and pressure decreases at many coastal East Antarctic stations during austral summer and autumn [*Turner et al.*, 2005]. Through geostrophic relationships, these pressure changes have caused shifts in the near-surface winds, which have been linked to changes in sea ice extent and concentration [*Turner et al.*, 2009; *Holland and Kwok*, 2012; *Meehl et al.*, 2016; *Purich et al.*, 2016], and the resulting changes in thermal advection have similarly been linked to ongoing warming across West Antarctica [*Steig et al.*, 2009; *Bromwich et al.*, 2013; *Nicolas and Bromwich*, 2014; *Clem and Fogt*, 2015] and the Antarctic Peninsula [*Clem and Fogt*, 2015; *Jones et al.*, 2016], as well as the lack of significant warming

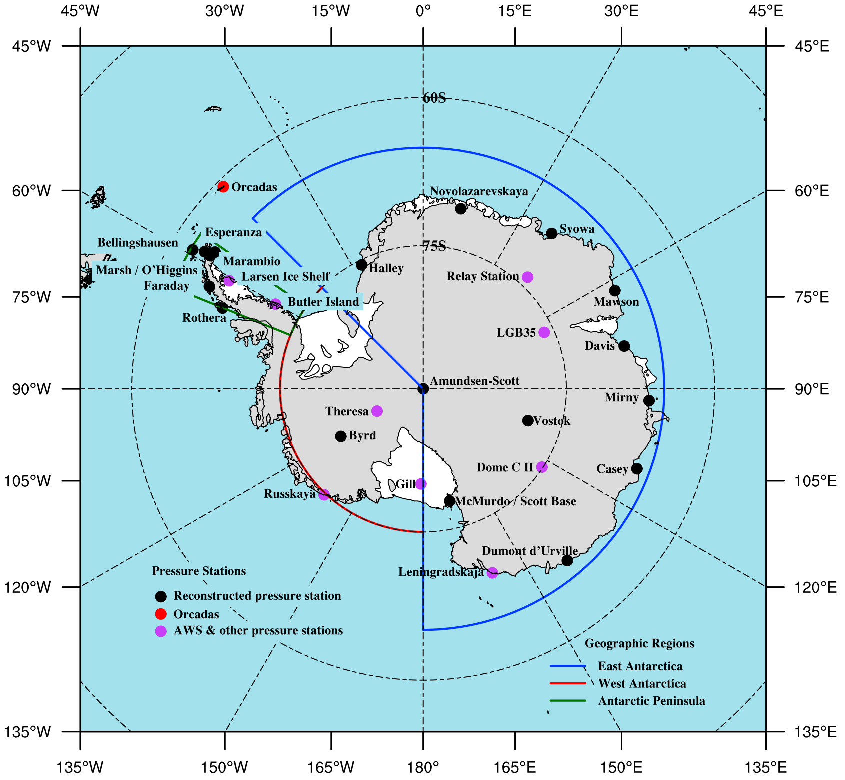

Figure 1. Displayed are the reconstructed station pressure locations (green), observations from Orcadas (red), and AWS locations (purple) used to create or evaluate (for AWS) the spatial Antarctic-wide pressure reconstruction. Outlined are the geographic regions used for further comparison, East Antarctica (45°W eastward to 180°, poleward of 66°S), West Antarctica (45°W westward to 180°, poleward of 75°S), and the Antarctic Peninsula (55°W–68°W, 62°S–75°S).

across much of East Antarctica [*Marshall*, 2007; *Steig et al.*, 2009; *Nicolas and Bromwich*, 2014] since the International Geophysical Year (IGY, 1957/1958). Unfortunately, very little is known about the full spatial pattern of atmospheric pressure prior to 1979, due largely to the fact that many gridded pressure data sets are unreliable prior to 1979 over the Antarctic [*Bromwich et al.*, 2007; *Bracegirdle and Marshall*, 2012], including those data sets that extend back throughout the early twentieth century [*Allan and Ansell*, 2006; *Jones and Lister*, 2007; *Compo et al.*, 2011; *Poli et al.*, 2016].

To provide a historical context for ongoing pressure changes at the major Antarctic research stations, a recent study reconstructed mean seasonal pressure at 18 stations across Antarctica (Figure 1) using midlatitude pressure data as predictors [*Fogt et al.*, 2016a, 2016b]. However, due to the large distances between the stations, these studies did not provide information about pressure across the entire Antarctic continent. Here we extend this earlier work by generating a new summer pressure reconstruction poleward of 60°S for the period 1905–2013 using these station reconstructions as anchoring points in a proven interpolation scheme and comprehensively evaluate the summer pressure variability and change across the entire Antarctic continent during the full twentieth century.

2. Data and Methods

2.1. Antarctic Pressure Data and Station Reconstructions

Monthly mean pressure records from staffed research stations and automatic weather stations are obtained from the Reference Antarctic Data for Environmental Research (READER; www.antarctica.ac.uk./met/READER) archive [*Turner et al.*, 2004] (see Figure 1 for locations). To extend the observations throughout the twentieth century at each station except Orcadas [*Zazulie et al.*, 2010], the summer station-based pressure reconstructions [*Fogt et al.*, 2016a, 2016b] were used. These reconstructions all have calibration correlations with observations greater than 0.75 and independent validation correlations with observations above 0.63; a full listing of the reconstruction performance at the 18 stations is given in supporting information Table S1. To generate and evaluate the spatial pressure reconstruction, the ERA-Interim reanalysis (ERA-Int) [*Dee et al.*, 2011] was used, which was shown to be the most reliable global reanalysis for Antarctic pressure [*Bracegirdle and Marshall*, 2012]. Austral summer (December–February) mean pressure was calculated from the observations and ERA-Int data. Further, since surface pressure varies widely across the Antarctic continent (due to large changes in elevation), all data sets were converted to surface pressure anomalies by removing the 1981–2010 climatological mean from the summer mean values.

2.2. Antarctic Spatial Pressure Reconstruction

The Antarctic spatial reconstruction is performed on a polar stereographic 80 km × 80 km Cartesian grid centered over the South Pole, and extending equatorward to 60°S, using the kriging method [*Cressie*, 1993; *Olea*, 1999] successfully employed for previous Antarctic surface temperature [*Monaghan et al.*, 2008; *Nicolas and Bromwich*, 2014] and snowfall [*Monaghan et al.*, 2006] reconstructions. The kriging weights are defined using ERA-Int reanalysis data during the model calibration period of 1979–2013 along with the 19 stations in Figure 1. As in *Nicolas and Bromwich* [2014], the kriging weights are optimized to avoid overfitting the model and are based on the covariances between the 19 stations used in the interpolation, and the relationship each of these stations have with each of the grid points on the Cartesian grid. Once the weights are determined, they are used in connection with the anomalies from the individual station pressure reconstructions [*Fogt et al.*, 2016a, 2016b] and the Orcadas observational record to produce a spatially complete surface pressure reconstruction over the Antarctic continent back to 1905. A separate validation of the spatial pressure reconstruction was performed by determining the kriging weights separately for the periods 1979–1996 and 1997–2013. These kriging weights are then used to produce an independent reconstruction for the withheld years. Combining the two predicted reconstructions produced in this manner yields the validation reconstruction.

2.3. Climate Model Simulations

We also investigate simulations from the Community Atmosphere Model, version 5 (CAM5) [*Neale et al.*, 2010], configured at a 0.9° latitude × 1.25° longitude horizontal resolution with a finite volume dynamical core and 26 vertical levels. Output from three ensembles of transient experiments with CAM5 is analyzed. The first ensemble, an ozone sensitivity experiment (here termed “Ozone Only”), is forced with time-varying ozone concentrations. In this experiment, SSTs, sea ice concentrations, and non-ozone radiative forcings are held to monthly varying climatologies. Ten ensemble members are integrated over the years 1900–2014, initialized from a preindustrial control simulation with each ensemble member receiving a random perturbation to the initial air temperature. The external forcings without time dependence beyond the seasonal cycle are set to climatological values for the year 1850. The second experiment has prescribed tropical sea surface temperatures, but all radiative forcings including ozone are held to monthly varying climatologies, set to preindustrial, 1850 values (termed “Tropical SSTs + Fixed Radiative”). Observed time-varying tropical SSTs are prescribed over 28°N–28°S, while a monthly varying climatology for SSTs and sea ice concentration is used poleward of 35°S. Between 28° and 35° in both hemispheres, the observed SST anomalies are tapered by adding damped anomalies (linearly weighted by latitude) to the climatologies. As in the first experiment, 10 ensemble members were integrated, initialized from a preindustrial control simulation with each ensemble member receiving a random perturbation to the initial air temperature. The second experiment covers the years 1874–2014. Note that this experiment does not purely separate internal variability from external forcing, as the tropical SSTs themselves have warmed slowly, likely in response to increasing greenhouse gasses. However, the impact of this slow warming on the extratropical circulation trends evaluated here is likely very small, as the main teleconnection patterns are generated by the anomalous east-west temperature gradients in the tropics and are largely expressed on interannual to decadal timescales. The final experiment prescribes sea ice and sea surface temperature the same as the second experiment but is forced by the full suite of time-varying radiative forcings (including ozone) plus tropical SSTs (termed Tropical SSTs + Radiative). Ten ensemble members were integrated over the 1880–2014, initialized from a preindustrial control simulation with each ensemble member receiving a random perturbation to the initial air temperature as before.

For all experiments, ozone forcing is from the Stratospheric-Tropospheric Processes and their Role in Climate (SPARC) data set [*Cionni et al.*, 2011; *Eyring et al.*, 2013]. The external forcing data sets besides ozone are consistent with the Coupled Model Intercomparison Project, Phase 5 (CMIP5) 20th Century Historical Experiment protocol [*Taylor et al.*, 2012]. For the fully forced experiment, values from the Representative Concentration

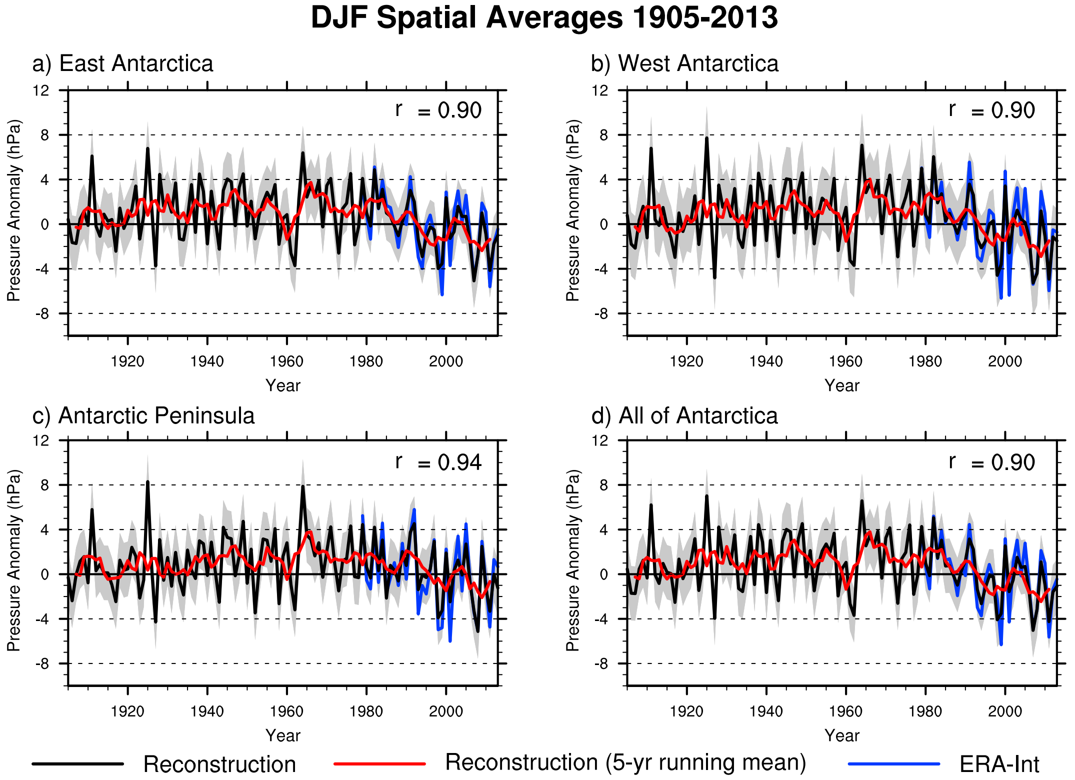

Figure 2. Pressure anomalies from the reconstruction (black, red with 5 year running mean) and 95% confidence intervals, along with ERA-Int pressure anomalies area averaged over the regions in Figure 1. (a) East Antarctica, (b) West Antarctica, (c) Antarctic Peninsula, and (d) All of the Antarctic continent (all regions in previous domains together). The 95% confidence intervals are evaluated as 1.96 times the standard deviation of the residuals based on the difference between the regionally averaged interannual reconstruction and ERA-Int surface pressure anomalies. Correlations of the reconstruction and ERA-Int area-averaged interannual pressure anomalies during 1979–2013 are given in each panel.

Pathway 8.5 [*van Vuuren et al.*, 2011] are used for the years 2006–2014. The SST and sea ice concentration boundary conditions are from the Extended Reconstruction of Sea Surface Temperature, version 4 (ERSSTv4) [*Huang et al.*, 2015], and the SST and sea ice concentration climatologies are based on the period 1880–2014; after 1950 ERSSTv4 is more strongly constrained by observations, especially in the high latitude oceans, and thus, the extratropical CAM5 climatological SSTs largely reflect the mean seasonal cycle after 1950 [*Huang et al.*, 2016].

2.4. Statistical Methods

Pearson product-moment correlations are used throughout the manuscript to assess the linear agreement between our reconstruction and various reanalysis products. We use two-tailed *t* tests to compare and assess statistical significance of mean pressure anomalies during two separate 30 year periods in the reconstruction; for observations, differences and their significance are only shown if the data are 75% complete. Trends are analyzed using least squares linear regression, and their statistical significance (and 95% confidence intervals) assessed using a *t* distribution.

3. Spatial Pressure Reconstruction Skill

The reconstruction skill is evaluated against the ERA-Interim Reanalysis (ERA-Int) [*Dee et al.*, 2011] in detail in supporting information Figure S1, and in all the following figures. Across the entire Antarctic continent, all skill measures evaluating the reconstruction but the coefficient of efficiency (CE) are above 0.70; for CE the entire continent is above 0.60 (Figure S1). These skill measures are considerably higher than for previous temperature reconstructions, which showed areas of negative CE [*Steig et al.*, 2009] or continental-averaged CE values (from monthly data) below 0.58 [*Nicolas and Bromwich*, 2014]. Skill metrics based on automatic weather station data (not used in generating kriging weights) all reveal similar high skill, although slightly lower at a few locations, most likely due to the shorter time intervals used for evaluation. The high reconstruction skill is attributed not only to the broad spatial homogeneity of summer mean surface pressure anomalies across Antarctica but also to the higher skills of the individual station-based pressure reconstructions in this season [*Fogt et al*., 2016a, 2016b] (supporting information Table S1).

4. Antarctic Pressure Changes During the Twentieth Century

With this new and reliable pressure data set, historical summer Antarctic pressure variability during the 20th century and early 21st century can be better understood in a longer context. We first analyze in Figure 2 regionally averaged surface pressure anomalies from the reconstruction and ERA-Int; for comparison, the regionally averaged surface pressure anomalies along with two other century length reanalyses are plotted in supporting information Figure S2. As in *Poli et al*. [2015], we find that other early twentieth century reanalysis products produce spurious pressure trends poleward of 60°S.

The regionally averaged surface pressure anomalies from the reconstruction agree very well with ERA-Int after 1979, with correlations greater than or equal to 0.90 for all regions. From this reconstruction, it is apparent that there are large and statistically significant negative pressure trends since around 1960, most marked in East and West Antarctica (Figures 2a and 2b). Prior to ~1960, area-averaged summer pressure anomalies in the reconstruction only twice exceeded +5 hPa, in 1925/1926 [*Fogt et al*., 2016b] and again in 1911/1912, the latter during the Amundsen and Scott race to the South Pole [*Fogt et al*., 2017]; all regions agree that when spatially averaged, Antarctica did not experience pressure anomalies below −5 hPa until the late 20th and early 21st century.

Pressure trends over different time periods are presented in Figure 3 (30 year epochal mean pressure differences produce similar results, supporting information Figure S3). Only in East Antarctica are the negative pressure trends during 1905–2013 significant at $p < 0.05$ (Figure 3a). The lack of statistical significance elsewhere is due to significant positive pressure trends across the southern Antarctic Peninsula and coastal South Atlantic sector in the early to middle portions of the twentieth century, as represented by trends in 1915–1974 (Figure 3b). When examining trends in the regionally averaged pressure for all possible lengths of at least 30 years (supporting information Figure S4), 1915–1974 corresponds to the only period of significant ($p < 0.10$) area-averaged positive trends in West Antarctica and the Antarctica Peninsula since 1905, although all regions show positive trends in the early twentieth century, indicating that the significant trends in Figure 3b are not entirely sensitive to the time period analyzed. Figure 3b does indicate stronger and more significant trends than supporting information Figure S4, as the region of significant trends occupies only portions of all three geographic regions used in area averaging, as seen in Figure 1. The regions of positive trends indicate a change in the summer polar vortex structure, likely caused by natural variability since they occur prior to the Antarctic ozone hole or strong changes in greenhouse gas concentrations, of which the latter has dominated Southern Hemisphere tropospheric circulation changes in the second half of the twentieth century [*Polvani et al*., 2011].

After 1957, negative pressure trends are seen everywhere across Antarctica, and our reconstruction aligns well with the observations (circles in Figures 3c and 3d), although the reconstruction trends (and therefore, the individual Antarctic station reconstructions that are interpolated) tend to be a bit stronger than observations in the Antarctic interior [cf. *Fogt et al*., 2016a, Figure 6a]. Spatially, the negative trends are the strongest from the southern Antarctic Peninsula eastward along the Antarctic coast to ~30°E, and also across the Ross Ice Shelf. The trend maps in Figures 3c and 3d indicate that the large negative trends seen in the area-averaged time series for West Antarctica (Figure 2b) are dominated by the coastal regions in the South Atlantic/Weddell Sea, whereas the smaller negative trend in the last 30 years for the Antarctic Peninsula (Figure 2c) is due to much weaker trends across the northern Antarctic Peninsula, in agreement with observations.

The temporal evolution of pressure trends for all of Antarctica is examined in Figure 3e, which displays the 30 year running trends in the reconstruction along with that from ERA-Int. Both the reconstruction and ERA-Int identify the late 20th and early 21st century summer Antarctic pressure trends as significantly different from zero at $p < 0.05$ (indicated by the gray shading), and also overall significantly more negative than any other 30 year running trend during the middle and early twentieth century. This suggests a unique aspect of Antarctic pressure decrease in the late twentieth century, which is dominated by the largest trends

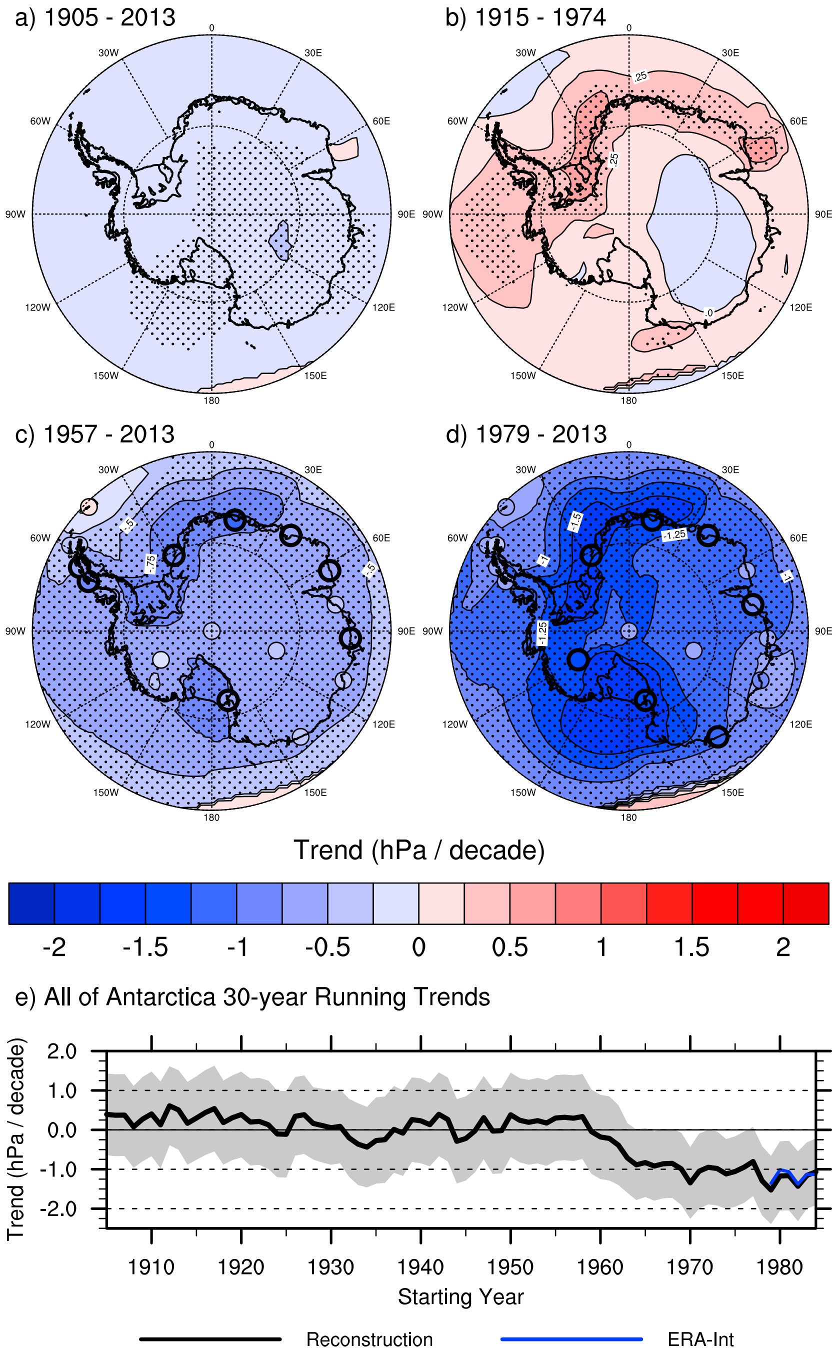

Figure 3. (a–d) Linear trends (hPa/decade) in summer pressure for different time periods; stippling indicates trends that are significantly different from zero at $p < 0.05$. Trends in station observations with >75% complete records are given in Figures 3c and 3d, with significant observed trends indicated by a thick outer black circle; although Byrd station in West Antarctica is <75% complete, it is still shown to represent trends in this region. (e) 30 year running trends (hPa decade^{-1}) of Antarctic-averaged surface pressure from the reconstruction (black) and ERA-Int (blue). The *x* axis in Figure 3c identifies the starting year of the 30 year trends, and the gray shading represents the 95% confidence interval for the reconstruction slope, based on a *t* distribution of the standard error of the regression coefficient.

occurring across the South Pacific and Atlantic sectors of Antarctica (Figures 3c and 3d). The region of recent strongest negative summer pressure trends along the coastal South Atlantic sector and Ross Ice Shelf is consistent with the summer pressure trends during 1971–2000 reported in *Turner et al.* [2005]; here we demonstrate spatially that these negative trends/pressure decreases are most marked along the coast and quickly weaken in the interior (especially during 1957–2013) and follow a period of positive pressure trends in the first half of the twentieth century.

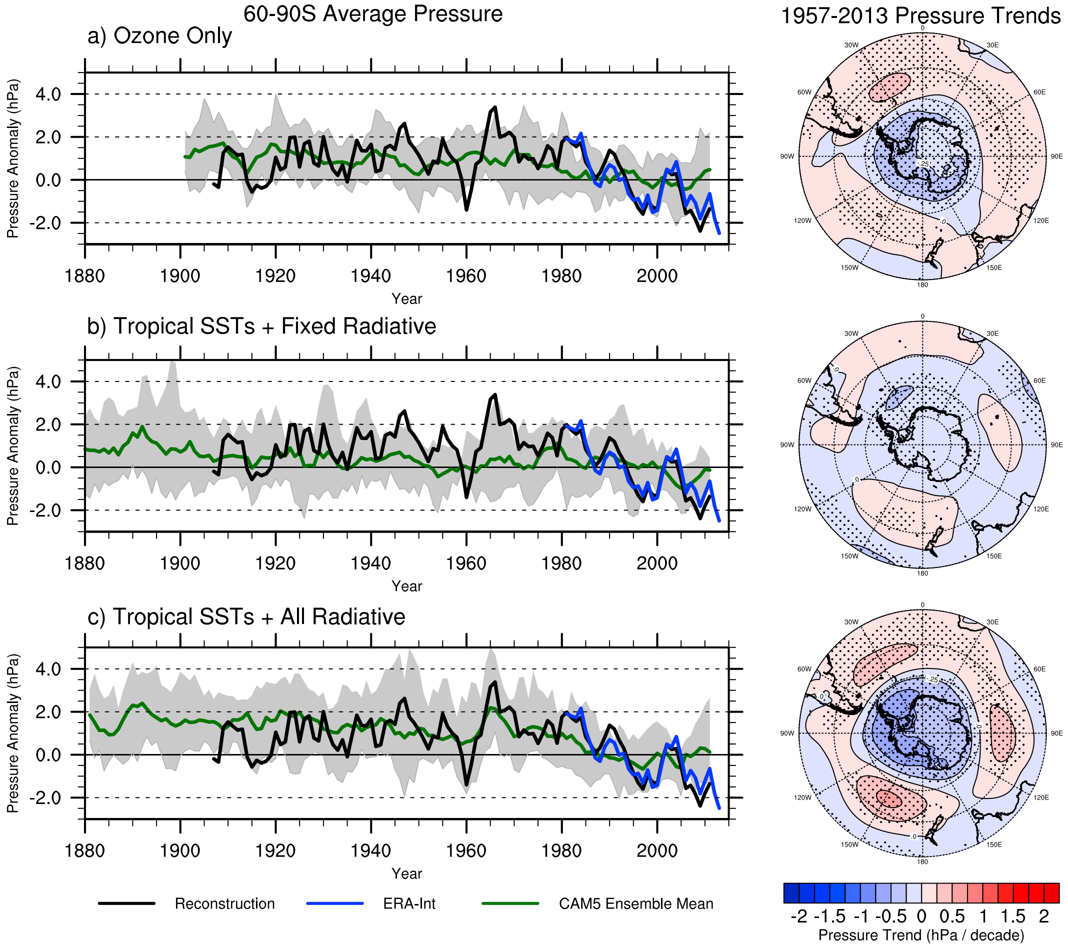

Figure 4. Comparison of 5 year running mean summer surface pressure anomalies (from the 1981–2010 average) from the reconstruction and ERA-Int, and CAM5 simulations, area averaged over 60°–90°S (left). The gray shading represents the full range of the 10 ensemble members (calculated after taking the 60–90°S averages) and the thick dark green line represents the CAM5 ensemble mean. Linear trends (hPa/decade) for the CAM5 ensemble means, as in Figure 3c, but poleward of 30°S (right). (a) CAM5 experiment with time-varying ozone only (other radiative forcings fixed) and climatological SSTs. (b) CAM5 experiment with prescribed tropical SSTs only and fixed radiative forcings. (c) CAM5 experiment with all radiative forcings plus prescribed tropical SSTs.

5. Interpretation of Antarctic Pressure Changes

To understand the causes of the pressure changes over the full twentieth century, we compare multiple ensemble simulations of CAM5 with the reconstructions in Figure 4, for both pressure averaged from 60 to 90°S (left) and spatial trends from 1957–2013 (right). Not only does our reconstruction compare well with ERA-Int after 1979 but also the reconstruction falls nearly completely in the range of the 10 ensemble members for all CAM5 simulations, highlighting the similar range of Antarctic pressure variability in these two data sets; this is not true when comparing CAM5 and our reconstruction with other reanalysis data sets across the twentieth century (supporting Figure S5), further highlighting issues in these reanalyses. Since there are still notable differences between the reconstruction and other gridded pressure data sets at 60°S, and the reconstruction skill is lower at 60°S than over the continent (supporting information Figure S1), we caution against the blending of the reconstruction with other gridded data sets north of 60°S (supporting information Figure S6).

Comparing the model simulations with the reconstructions indicates that ozone forcing, the commonly attributed mechanism for the recent summer pressure trends [*Thompson and Solomon*, 2002; *Arblaster and Meehl*, 2006; *Miller et al*., 2006; *Fogt et al*., 2009], explains a large portion of the negative pressure trends poleward of 60°S since 1957, in agreement with *Polvani et al*. [2011]. In Figure 4a, throughout all but the very late twentieth century, the Ozone Only ensemble mean pressure is above 0 hPa and only begins to decline noticeably after 1970; it continues to decrease after 1990, consistently having negative pressure anomalies during 2000–2010, with a few ensemble members showing pressure anomalies <-1.5 hPa at this time, consistent with the reconstruction and ERA-Int. Spatially, significant negative pressure trends are observed across the entire Antarctic continent (Figure 4a, right), in a positive SAM structure. Nonetheless, the Ozone Only experiment does not fully capture the negative trend (Figure 4a), especially when trends are examined after 1979. After 1979, the Ozone Only ensemble mean reveals a similar trend pattern as in Figure 4a, but none of the trends are statistically significant poleward of 60°S (supporting information Figure S7a). While smaller in magnitude from 1957 to 2013, the Tropical SSTs + Fixed Radiative experiment also shows negative pressure trends, which are significant in the South Atlantic sector of Antarctica, in agreement with observations and our reconstruction (Figure 3c). Importantly, the Tropical SSTs + Fixed Radiative experiment has even lower pressure anomalies in the ensemble mean after 2000, and these anomalies never rise again above 0 hPa (Figure 4b), whereas they become positive again in the Ozone Only experiment after 2010 (Figure 4a). In turn, the negative pressure trends are even stronger in the Tropical SSTs + Fixed Radiative experiment after 1979 (supporting information Figure S7b), with the strongest negative trends located in the South Pacific sector, the region of strongest tropical teleconnections in Antarctica [*Turner*, 2004]. As such, it is very likely that a portion of the observed negative trend since 1960 is due in part to tropical SST variability and trends by generating sharply negative pressure anomalies after 2000. Across the entire twentieth century, Figure 4b suggests that tropical SSTs have not contributed substantially to long-term, Antarctic-wide pressure trends but have had an influence on decadal timescales, most notably contributing to negative pressure anomalies after the year 2000. Other work [*Staten et al*., 2012] has suggested that warming tropical SSTs have contributed to Antarctic pressure and wind trends during the twentieth century, perhaps playing as large a role as ozone depletion. Similarly, additional studies [*Li et al*., 2014; *Meehl et al*., 2016; *Purich et al*., 2016] have demonstrated that decadal-scale tropical SST variability is an important mechanism to explaining changes not only in the high southern latitude atmospheric circulation [*Clem and Fogt*, 2015; *Schneider et al*., 2015; *Jones et al*., 2016] but also in Antarctic sea ice. Detrended correlations during 1905–2013 between ERSSTv4 and pressure averaged 60°–90°S in the reconstruction and CAM5 simulations with tropical SSTs all agree that the strongest tropical SST relationships with Antarctic pressure are found in the tropical Pacific, with perhaps a weaker signal in the tropical Atlantic (supporting information Figure S8).

Not surprisingly, the combination of tropical SSTs and all radiative forcings produces the best match with the reconstruction and ERA-Int and has the strongest trend in the late 20th and early 21st century (Figure 4c). The trend pattern in this experiment (Figure 4c, right) also aligns well with the overall pattern in our reconstruction and observations (Figure 3c), indicating that both ozone depletion and tropical SST variability (especially after 1979) are leading to the strongest trends being observed across the South Atlantic and South Pacific sectors of Antarctica. Furthermore, part of the better agreement between the Tropical SSTs + Radiative ensemble mean and the reconstruction stems from the higher pressure anomalies in this experiment in the late 1960s (Figure 4c), which is also seen in other reanalysis data sets (supporting information Figure S5), and immediately follows marked low-pressure anomalies in 1961–1962. The higher-pressure values in the late 1960s are not present in the Ozone Only (Figure 4a) or Tropical SSTs + Fixed Radiative experiments (Figure 4b), suggesting that they are a result of a separate radiative forcing mechanism apart from stratospheric ozone depletion; our modeling experiments indicate that this is a robust forced response, as all ensemble members in the Tropical SSTs + All Radiative experiment show positive pressure anomalies at this time (Figure 4c). Earlier work has suggested that this peak, and the corresponding negative value in the SAM index, may be partly influenced by the Agung volcanic eruption in February of 1963 [*Marshall*, 2003]. Further analysis to isolate the various processes shows that radiative forcing apart from ozone depletion is the only forcing mechanism to reveal a spike in Antarctic-averaged pressure anomalies in the late 1960s (supporting information Figure S9f). The combination of tropical SST variability and ozone depletion (a linear addition of the ensemble means in Figures 4a and 4b, without any additional radiative forcings) produces a trend that captures most of the signal in the Tropical SSTs + All Radiative experiment but lacks the relatively high pressure anomalies in the late 1960s (supporting information Figure S9d).

6. Conclusions

A newly generated reliable summer pressure reconstruction across Antarctica since 1905 demonstrates that only across East Antarctica are the recent pressure trends unique when viewed in the context of the full twentieth century. In the coastal Atlantic sector of West Antarctica, pressures were similarly low in the early twentieth century and, when combined with higher pressure anomalies in the middle twentieth century, give rise to significant positive pressure trends in much of the early twentieth century in this region, which are likely caused by natural variability prior to the period of Antarctic stratospheric ozone depletion. When examining causality of the Antarctic pressure variability and change in a suite of climate model experiments in the context of the full twentieth century, it becomes clear that multiple influences in addition to ozone depletion have had a pronounced impact on Antarctic summer pressure variability, especially in the last 60 years. As the negative summer pressure trends are ubiquitous across Antarctica after 1957 in our reconstruction and observations and project strongly onto a positive SAM pattern, we therefore also suggest that multiple influences in addition to ozone depletion lead to the positive trend in the summer SAM index since 1957. Tropical SST variability has likely played a role in negative pressure anomalies across Antarctica in the last 15 years, perhaps timed with the shift of the Pacific Decadal Oscillation/Interdecadal Pacific Oscillation [*Clem and Fogt*, 2015; *Meehl et al.*, 2016; *Purich et al.*, 2016]; other recent modeling work further highlights the importance of the tropical SSTs compared to ozone depletion after 1979 on the changes in the 850 hPa zonal winds [*Schneider et al.*, 2015]. Our work also suggests that volcanic activity or other radiative forcing mechanisms played an important role in generating positive summer pressure anomalies in the late 1960s across Antarctica that contribute to the negative pressure trend in the last 60 years. Future work motivated by the seasonal Antarctic pressure reconstructions in comparison with model simulations and estimates of tropical SST variability will hopefully further improve the understanding of 20th century Antarctic climate variability, especially in other seasons outside austral summer where Antarctic atmospheric circulation trends appear more likely related to natural processes [*Jones et al.*, 2016].

Acknowledgments

Data from both the station-based and spatial pressure reconstructions are available from figshare at the following URLs: https://doi.org/10.6084/m9.figshare.3412813 (station reconstructions) and https://doi.org/10.6084/m9.figshare.5325541 (spatial reconstructions). Data for the climate model simulations may be downloaded from http://www.cesm.ucar.edu/experiments/cesm1.1/LE, or by contacting the authors. R.L.F., C.A.G., and H.E.D. acknowledge support from the National Science Foundation (NSF), grant PLR-1341621, while D.P.S. acknowledges support from NSF grant PLR-1341527. D.H.B. and J.P.N. acknowledge support from NSF grant PLR-1341695. The Climate Variability and Change Working Group of the Community Earth System Model led the production of the CAM5 experiments with time-varying tropical SSTs and time-varying radiative forcing. Contribution 1572 of Byrd Polar and Climate Research Center.

References

Allan, R., and T. Ansell (2006), A new globally complete monthly historical gridded mean sea level pressure dataset (HadSLP2): 1850–2004, *J. Clim.*, *19*(22), 5816–5842.

Arblaster, J. M., and G. A. Meehl (2006), Contributions of external forcings to southern annular mode trends, *J. Clim.*, *19*(12), 2896–2905.

Bracegirdle, T. J., and G. J. Marshall (2012), The reliability of Antarctic tropospheric pressure and temperature in the latest global reanalyses, *J. Clim.*, *25*(20), 7138–7146, doi:10.1175/JCLI-D-11-00685.1.

Bromwich, D. H., R. L. Fogt, K. I. Hodges, and J. E. Walsh (2007), A tropospheric assessment of the ERA-40, NCEP, and JRA-25 global reanalyses in the polar regions, *J. Geophys. Res.*, *112*, D10111, doi:10.1029/2006JD007859.

Bromwich, D. H., J. P. Nicolas, A. J. Monaghan, M. A. Lazzara, L. M. Keller, G. A. Weidner, and A. B. Wilson (2013), Corrigendum: Central West Antarctica among the most rapidly warming regions on Earth, *Nat. Geosci.*, *7*(1), 76–76, doi:10.1038/ngeo2016.

Cionni, I., V. Eyring, J. F. Lamarque, W. J. Randel, D. S. Stevenson, F. Wu, G. E. Bodeker, T. G. Shepherd, D. T. Shindell, and D. W. Waugh (2011), Ozone database in support of CMIP5 simulations: Results and corresponding radiative forcing, *Atmos. Chem. Phys.*, *11*(21), 11,267–11,292, doi:10.5194/acp-11-11267-2011.

Clem, K. R., and R. L. Fogt (2015), South Pacific circulation changes and their connection to the tropics and regional Antarctic warming in austral spring, 1979–2012, *J. Geophys. Res. Atmos.*, *120*, 2773–2792, doi:10.1002/2014JD022940.

Compo, G. P., et al. (2011), The twentieth century reanalysis project, *Q. J. R. Meteorol. Soc.*, *137*(654), 1–28, doi:10.1002/qj.776.

Cressie, N. A. C. (1993), *Statistics for Spatial Data: Cressie/Statistics*, *Wiley Series in Probability and Statistics*, John Wiley, Hoboken, N. J.

Dee, D. P., et al. (2011), The ERA-Interim reanalysis: Configuration and performance of the data assimilation system, *Q. J. R. Meteorol. Soc.*, *137*(656), 553–597, doi:10.1002/qj.828.

England, M. R., L. M. Polvani, K. L. Smith, L. Landrum, and M. M. Holland (2016), Robust response of the Amundsen Sea Low to stratospheric ozone depletion, *Geophys. Res. Lett.*, *43*, 8207–8213, doi:10.1002/2016GL070055.

Eyring, V., et al. (2013), Long-term ozone changes and associated climate impacts in CMIP5 simulations, *J. Geophys. Res. Atmos.*, *118*, 5029–5060, doi:10.1002/jgrd.50316.

Fogt, R. L., and A. J. Wovrosh (2015), The relative influence of tropical sea surface temperatures and radiative forcing on the Amundsen Sea Low, *J. Clim.*, *28*(21), 8540–8555, doi:10.1175/JCLI-D-15-0091.1.

Fogt, R. L., and E. A. Zbacnik (2014), Sensitivity of the Amundsen Sea Low to stratospheric ozone depletion, *J. Clim.*, *27*(24), 9383–9400, doi:10.1175/JCLI-D-13-00657.1.

Fogt, R. L., J. Perlwitz, A. J. Monaghan, D. H. Bromwich, J. M. Jones, and G. J. Marshall (2009), Historical SAM variability. Part II: Twentieth-century variability and trends from reconstructions, observations, and the IPCC AR4 models*, *J. Clim.*, *22*(20), 5346–5365, doi:10.1175/2009JCLI2786.1.

Fogt, R. L., C. A. Goergens, M. E. Jones, G. A. Witte, M. Y. Lee, and J. M. Jones (2016a), Antarctic station-based seasonal pressure reconstructions since 1905: 1. Reconstruction evaluation, *J. Geophys. Res. Atmos.*, *121*, 2814–2835, doi:10.1002/2015JD024564.

Fogt, R. L., J. M. Jones, C. A. Goergens, M. E. Jones, G. A. Witte, and M. Y. Lee (2016b), Antarctic station-based seasonal pressure reconstructions since 1905: 2. Variability and trends during the twentieth century, *J. Geophys. Res. Atmos.*, *121*, 2836–2856, doi:10.1002/2015JD024565.

Fogt, R. L., M. E. Jones, S. Solomon, J. M. Jones, and C. A. Goergens (2017), An exceptional summer during the South Pole race of 1911–1912, *Bull. Am. Meteorol. Soc.*, doi:10.1175/BAMS-D-17-0013.1.

Holland, P. R., and R. Kwok (2012), Wind-driven trends in Antarctic sea-ice drift, *Nat. Geosci.*, *5*(12), 872–875, doi:10.1038/ngeo1627.

Huang, B., V. F. Banzon, E. Freeman, J. Lawrimore, W. Liu, T. C. Peterson, T. M. Smith, P. W. Thorne, S. D. Woodruff, and H.-M. Zhang (2015), Extended Reconstructed Sea urface Temperature version 4 (ERSST.v4). Part I: Upgrades and intercomparisons, *J. Clim.*, *28*(3), 911–930, doi:10.1175/JCLI-D-14-00006.1.

Huang, B., P. W. Thorne, T. M. Smith, W. Liu, J. Lawrimore, V. F. Banzon, H.-M. Zhang, T. C. Peterson, and M. Menne (2016), Further exploring and quantifying uncertainties for Extended Reconstructed Sea Surface Temperature (ERSST) version 4 (v4), *J. Clim.*, *29*(9), 3119–3142, doi:10.1175/JCLI-D-15-0430.1.

Jones, J. M., et al. (2016), Assessing recent trends in high-latitude Southern Hemisphere surface climate, *Nat. Clim. Change*, *6*(10), 917–926, doi:10.1038/nclimate3103.

Jones, P. D., and D. H. Lister (2007), Intercomparison of four different Southern Hemisphere sea level pressure datasets, *Geophys. Res. Lett.*, *34*, L10704, doi:10.1029/2007GL029251.

Li, X., D. M. Holland, E. P. Gerber, and C. Yoo (2014), Impacts of the north and tropical Atlantic Ocean on the Antarctic Peninsula and sea ice, *Nature*, *505*(7484), 538–542, doi:10.1038/nature12945.

Marshall, G. J. (2003), Trends in the southern annular mode from observations and reanalyses, *J. Clim.*, *16*(24), 4134–4143, doi:10.1175/1520-0442(2003)016<4134:TITSAM>2.0.CO;2.

Marshall, G. J. (2007), Half-century seasonal relationships between the Southern Annular Mode and Antarctic temperatures, *Int. J. Climatol.*, *27*(3), 373–383, doi:10.1002/joc.1407.

Meehl, G. A., J. M. Arblaster, C. M. Bitz, C. T. Y. Chung, and H. Teng (2016), Antarctic sea-ice expansion between 2000 and 2014 driven by tropical Pacific decadal climate variability, *Nat. Geosci.*, *9*(8), 590–595, doi:10.1038/ngeo2751.

Miller, R. L., G. A. Schmidt, and D. T. Shindell (2006), Forced annular variations in the 20th century Intergovernmental Panel on Climate Change Fourth Assessment Report models, *J. Geophys. Res.*, *111*, D18101, doi:10.1029/2005JD006323.

Monaghan, A. J., et al. (2006), Insignificant change in Antarctic snowfall since the International Geophysical Year, *Science*, *313*(5788), 827–831, doi:10.1126/science.1128243.

Monaghan, A. J., D. H. Bromwich, W. Chapman, and J. C. Comiso (2008), Recent variability and trends of Antarctic near-surface temperature, *J. Geophys. Res.*, *113*, D04105, doi:10.1029/2007JD009094.

Neale, R. B., et al. (2010), Description of the NCAR Community Atmosphere Model (CAM5.0), NCAR.

Nicolas, J. P., and D. H. Bromwich (2014), New reconstruction of Antarctic near-surface temperatures: Multidecadal trends and reliability of global reanalyses, *J. Clim.*, *27*(21), 8070–8093, doi:10.1175/JCLI-D-13-00733.1.

Olea, R. A. (1999), *Geostatistics for Engineers and Earth Scientists*, Springer Science+Business Media, LLC, New York.

Poli, P., H. Hersbach, P. Berrisford, D. Dee, A. J. Simmons, and P. Laloyaux (2015), ERA-20C deterministic, ERA Rep. Ser., ECMWF.

Poli, P., et al. (2016), ERA-20C: An atmospheric reanalysis of the twentieth century, *J. Clim.*, *29*(11), 4083–4097, doi:10.1175/JCLI-D-15-0556.1.

Polvani, L. M., D. W. Waugh, G. J. P. Correa, and S.-W. Son (2011), Stratospheric ozone depletion: The main driver of twentieth-century atmospheric circulation changes in the Southern Hemisphere, *J. Clim.*, *24*(3), 795–812, doi:10.1175/2010JCLI3772.1.

Purich, A., M. H. England, W. Cai, Y. Chikamoto, A. Timmermann, J. C. Fyfe, L. Frankcombe, G. A. Meehl, and J. M. Arblaster (2016), Tropical Pacific SST drivers of recent Antarctic Sea ice trends, *J. Clim.*, *29*(24), 8931–8948, doi:10.1175/JCLI-D-16-0440.1.

Raphael, M. N., G. J. Marshall, J. Turner, R. L. Fogt, D. Schneider, D. A. Dixon, J. S. Hosking, J. M. Jones, and W. R. Hobbs (2016), The Amundsen Sea Low: Variability, change, and impact on Antarctic climate, *Bull. Am. Meteorol. Soc.*, *97*(1), 111–121, doi:10.1175/BAMS-D-14-00018.1.

Schneider, D. P., C. Deser, and T. Fan (2015), Comparing the impacts of tropical SST variability and polar stratospheric ozone loss on the Southern Ocean westerly winds, *J. Clim.*, *28*(23), 9350–9372, doi:10.1175/JCLI-D-15-0090.1.

Staten, P. W., J. J. Rutz, T. Reichler, and J. Lu (2012), Breaking down the tropospheric circulation response by forcing, *Clim. Dyn.*, *39*(9–10), 2361–2375, doi:10.1007/s00382-011-1267-y.

Steig, E. J., D. P. Schneider, S. D. Rutherford, M. E. Mann, J. C. Comiso, and D. T. Shindell (2009), Warming of the Antarctic ice-sheet surface since the 1957 International Geophysical Year, *Nature*, *457*(7228), 459–462, doi:10.1038/nature07669.

Taylor, K. E., R. J. Stouffer, and G. A. Meehl (2012), An overview of CMIP5 and the experiment design, *Bull. Am. Meteorol. Soc.*, *93*(4), 485–498, doi:10.1175/BAMS-D-11-00094.1.

Thompson, D. W. J., and S. Solomon (2002), Interpretation of recent Southern Hemisphere climate change, *Science*, *296*(5569), 895–899, doi:10.1126/science.1069270.

Turner, J. (2004), The El Niño–Southern Oscillation and Antarctica, *Int. J. Climatol.*, *24*(1), 1–31, doi:10.1002/joc.965.

Turner, J., S. R. Colwell, G. J. Marshall, T. A. Lachlan-Cope, A. M. Carleton, P. D. Jones, V. Lagun, P. A. Reid, and S. Iagovkina (2004), The SCAR READER project: Toward a high-quality database of mean Antarctic meteorological observations, *J. Clim.*, *17*(14), 2890–2898, doi:10.1175/1520-0442(2004)017<2890:TSRPTA>2.0.CO;2.

Turner, J., S. R. Colwell, G. J. Marshall, T. A. Lachlan-Cope, A. M. Carleton, P. D. Jones, V. Lagun, P. A. Reid, and S. Iagovkina (2005), Antarctic climate change during the last 50 years, *Int. J. Climatol.*, *25*(3), 279–294, doi:10.1002/joc.1130.

Turner, J., J. C. Comiso, G. J. Marshall, T. A. Lachlan-Cope, T. Bracegirdle, T. Maksym, M. P. Meredith, Z. Wang, and A. Orr (2009), Non-annular atmospheric circulation change induced by stratospheric ozone depletion and its role in the recent increase of Antarctic sea ice extent, *Geophys. Res. Lett.*, *36*, L08502, doi:10.1029/2009GL037524.

Turner, J., T. J. Bracegirdle, T. Phillips, G. J. Marshall, and J. S. Hosking (2013), An initial assessment of Antarctic Sea ice extent in the CMIP5 models, *J. Clim.*, *26*(5), 1473–1484, doi:10.1175/JCLI-D-12-00068.1.

van Vuuren, D. P., et al. (2011), The representative concentration pathways: An overview, *Clim. Change*, *109*(1–2), 5–31, doi:10.1007/s10584-011-0148-z.

Zazulie, N., M. Rusticucci, and S. Solomon (2010), Changes in climate at high southern latitudes: A unique daily record at Orcadas spanning 1903–2008, *J. Clim.*, *23*(1), 189–196, doi:10.1175/2009JCLI3074.1.